DRAFT VERSION MAY 6, 2025
Typeset using LaTeX **twocolumn** style in AASTeX631

Creating a Color-Magnitude Diagram for Open Cluster Mel 71

RAUL LAMA,[1] JACQUELINE VAZQUEZ,[1] PAULINA SHIRASHI,[1] AND ARIYANA BONAB[1]

[1]*Department of Astronomy, Boston University, 725 Commonwealth Ave., Boston, MA 02215, USA*

ABSTRACT

In studying the properties of hundreds to thousands of stars at a time, the Hertzsprung–Russell diagram (HRD) is an indispensable resource for astronomers. The form of this diagram that is most important for our work is the color-magnitude diagram (CMD) which allows us to study star clusters. In this lab, we observe and study the open cluster Mel 71 with the Perkins Telescope and its primary optical instrument PRISM in order to produce an accurate CMD. After calibrating multiple images of the cluster in the B,V, and R filters, we look to measure the apparent magnitudes and B-V colors of each star after confirming their cluster membership. Plotting these two values against each other for a total of 393 cluster stars, we obtain an accurate CMD that reports a main sequence turnoff point at $(B-V) = 0.35$ and apparent V magnitude of 13. We also take note of a branch of red giants in the diagram from $(B-V) = 0.6, V = 13$ to $(B-V) = 1.2, V = 10$. Our CMD allows us to confirm that Mel 71 is in fact an open cluster and we now have information of the evolution stage of each plotted star that we may use in any future research into this cluster.

1. INTRODUCTION

Rather than forming in isolation, most stars form in clusters, which are collections of gravitationally-bound stars birthed from the same cloud of interstellar gas and dust.[1] There are two categories of star clusters: open clusters and globular clusters. Open clusters, which are most important to our work, are composed of between ten to a few thousand loosely-bound, young stars. These clusters are significantly less dense than their globular counterparts, making it much easier to resolve each cluster member with a telescope and do any necessary photometry on them.[2]

These star clusters are essential in understanding stellar evolution. Due to the shared origin of stars in a cluster, we may generally assume that they have similar chemical compositions, ages, and distances from Earth, but different masses.[3] Further, since more massive stars evolve quicker than lower mass stars, each star in a cluster will be at a different stage of their evolution. These properties, in turn, allow astronomers to study the effects of stellar evolution on these cluster stars by observing the star cluster at a single point in time. This work produces an isochrone—the relationship between temperature and brightness of stars in the same cluster—that acts as a microcosm for the general evolution of stars.[4]

[1] Harvard and Smithsonian Center for Astrophysics, Star Clusters
[2] Australia Telescope National Facility, Open Star Clusters
[3] GAIA in the UK, Star clusters: observing the effects of stellar evolution
[4] Ibid.

To quantify this relationship, we use color-magnitude diagrams (CMD), which are a variant of the Hertzsprung–Russell diagram (HRD). Typically, HRDs visually represent the different stages of stellar evolution by plotting the absolute magnitudes and spectral types of many individual stars. CMDs, which plot the apparent magnitudes against the color index of stars, instead illustrate the effects of evolution on similar age stars with different masses in a star cluster.

In this lab, in order to create an accurate CMD, we observe the open cluster Mel 71 with the Perkins Telescope's PRISM instrument. Below is some useful information about the cluster:[5]

1. Right Ascension (RA) ($ep = J2000$): $07^h37^m31.9^s$
2. Declination (DEC) ($ep = J2000$): -12°03′54″
3. Approx. Distance: 3060 pc
4. Diameter: 8 $arcmin$
5. Age: 930 Myr

We first take and calibrate multiple images of Mel 71 in the B, V, and R filters. Then, we do a star query on the images using an astronomical database, such as SIMBAD, in order to obtain the necessary information of the stars pictured. It is important to note that not all of the stars in our images

[5] SIMAD and Open Clusters

are part of the cluster. To address this issue, we use similar proper motion values as a requirement for cluster membership. Since stars in the same cluster are gravitationally-bound, they will move at similar speeds. After filtering out the non-members, we then perform aperture photometry on each star to obtain apparent magnitudes in the B and V bands. Stars in a open cluster are spread out and are all at roughly the same distance from an observer on Earth, so we are able to measure their apparent magnitudes accurately with our method. After we do this for the B and V bands, we then obtain the $(B - V)$ color index for each star by simply subtracting the B and V apparent magnitudes. Color index is the difference of a star's magnitude in two different filters. The lower a star's color index is, the bluer and hotter it is. With both V and $(B - V)$ for all of our cluster stars, we then simply plot them against each other to create a CMD.

While the choice of Mel 71 has no scientific reasoning behind it, a motivator for our work is that the last photometric study done on this cluster was in 1985 by Marc W. Pound and Kenneth A. Janes. We find it important to produce an updated CMD given that we have access to better data and processing techniques. Further, our new CMD gives us accurate information for the effect of stellar evolution on the stars in Mel 71 that we, and other astronomers, can use for further research.

2. OBSERVATIONS

All of the observations of Mel 71 in this lab are done using the Perkins Re-Imaging SysteM (PRISM) optical instrument for the Perkins telescope operated at the Perkins Telescope Observatory in Flagstaff, Arizona. The important specifications of PRISM and the telescope are the following:[6]

1. CCD field of view: 13.65 x 13.65 $arcmin$
2. CCD pixel scale: 0.39 $arcsec\, pixel^{-1}$
3. Telescope primary diameter: 72 in (1.83 m)
4. Telescope primary F/#: 4.18

Due to less than ideal observing conditions on 3/18/24 UTC as a result of high humidity from snow and rain, we are not able to obtain any science images of Mel 71. Instead, we take our calibration images. First we take 11 bias images, instrument cover on, with an average of about 1100 counts. Then, we take flat field images in the B, V, and R filters. For each filter, we first illuminate a screen in front of the telescope and then remove the cover. For the V and R filters, we take six 6 s exposure flats. We note that PRISM saturates at $65,000$ counts and pixels on the flats have counts between 20 to $30,000$ due to overscan regions and dust. For the B filter, we take five 50 s exposure flats. Since the quantum efficiency of the blue chip in PRISM is worse, we need longer exposure times to get the same counts as the V and R flats. Note that the operating temperature of PRISM is -112.36° C, so dark current is not a source of noise in our science images.

On 3/21/24 UTC, we remotely observe Mel 71 and take 17 images in total. At 03:17, we begin taking images in the V band. Cloud coverage is about 10%, humidity at 73%, airmass of 1.5, and temperature at $4.6°$ C. The seeing throughout the night is not ideal, at about 2.9 $arcsec$. With the dome open, we take images in the V, B, and R filters in that order. The optimal telescope focus for the V band is 3700, 3630 for the B band, and 3690 for the R band. In the V filter, we take three 30 s and two 60 s exposures. For the B filter, we take three 60 s and two 120 s exposures. In the R filter, we take two 30 s exposures, two 60 s exposures, and three 120 s exposures. We end our observations of Mel 71 at roughly 03:45. Note that, for the purposes of our work, we largely ignore the observations done in the R band.

3. ANALYSIS

3.1. *Science Image Calibration*

Prior to doing any actual science, it is important to lay out our calibration process for each image analyzed for the purposes of this lab. Note that this process is the exact same for each image taken, with the only differences being in the filters and exposure times. We use python to do all of our image calibration and analysis, with the software listed in the section 5.

First, for convenience, we define a function that displays any inputted image. Next, to get the best possible calibration images, we take steps to create a primary bias image and primary flats in each filter through batch processing. With this method, we separate the biases, flats, and science images by filter into their own folders. Then, we read in the biases and create a stack of the data from the 11 images. We clip them to make a subframe in order to get rid of the overscan regions that we will have to deal with in the future. Note that the size of the overscan regions will vary depending on the CCD. It is critical that the clipping does not affect or cutoff the objects being observed. To obtain our primary bias image, we take the median array of the stacked bias image data and save it.

The process for the flat field images is the same in each filter. After reading in all of the flats, we create a stack of their data and clip them accordingly to get rid of overscan. Note that the clipping for each image we work with is the same in order to maintain shape consistency. We then subtract our primary bias from each flat in the stack and then divide by their respective median counts in order to normalize them. Next, we take the median array of these stacked, normalized

[6] Boston University, Perkins Observatory Instruments

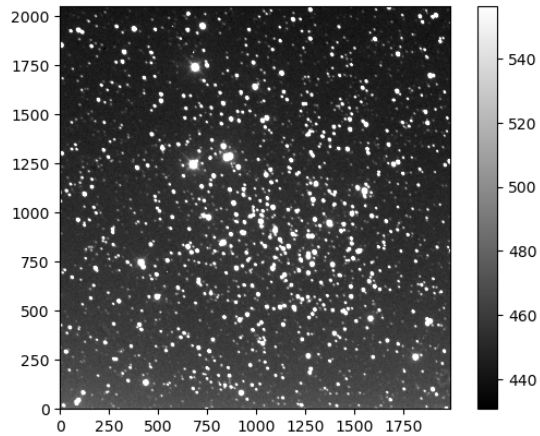

Figure 1. Calibrated 60 s exposure of Mel 71 in the V filter. Note that the orientation is flipped compared to finder charts such as Aladin, with North down, East right.

flats and then divide that by its median in order to get our primary flat field images.

With the primary bias and flats in each filter, we calibrate our raw science images. Note that the process is the same for each image, making sure that we use the flats that have the same filter and exposure time as the raw images. For example, with the V band images, we clip them the same as the bias and flats and then subtract the primary bias from this subframe to perform a bias correction. We then divide this image by our primary V band flat to complete the calibration and then save the images for further processing. An example of a calibrated image we analyze in this lab is pictured in Figure 1.

3.2. *SIMBAD Query*

To identify the stars in the frame of our images, we take one image, such as the one in Figure 1, and perform an astroquery. In particular, we query a circular region of radius 350 $arsec$ around the star Cl* Mel 71 MMU 130 using the SIMBAD database to obtain the RAs, DECs, and proper motions in $mas\ yr^{-1}$ of stars in the region. We take MMU 130 [RA($J2000$) = $07^h37^m30.05^s$, DEC(J2000) = -$12°04'23.53''$] as the origin of the query region because it is close to the center of the cluster. It is important the we turn MMU 130's location into a SkyCoord object to use for the query, otherwise this method will not work. Note that when querying SIMBAD, we have to tell the query what information we want it to extract. Since we want the proper motions of stars, we have to add another field of search denoted by the keyword "mespm." Once the query is done, we obtain the relevant information of 456 stars and save the data as a table to further analyze. The region of the sky that we query is pictured in Figure 2.

3.3. *Cluster Membership*

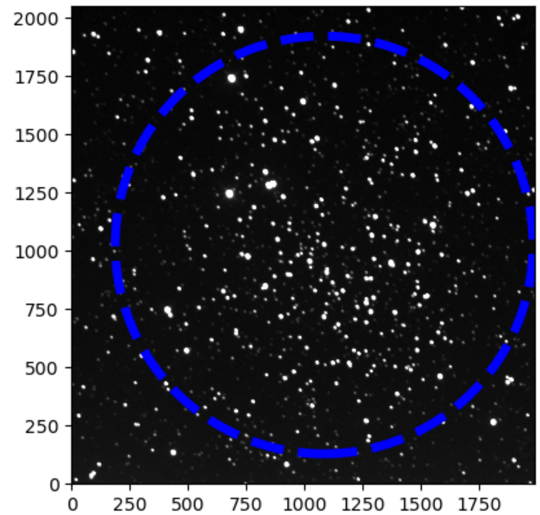

Figure 2. Query region of 350 $arsec$ around MMU 130 on the calibrated 60 s exposure of Mel 71 in the V filter. Note that the orientation is North down, East right.

Not every star in the query region is a member of Mel 71, so it is necessary to devise some method to determine cluster membership. For our work, we use the proper motion of the queried stars as a criteria since stars in the same cluster move at similar speeds. To do so, we first extract the proper motions, labelled "PM_pmra," from our query. We then take the mean of the proper motions, which we find to be -2.36 $mas\ yr^{-1}$. With this average value, we define a deviation of $\pm 0.5\ mas\ yr^{-1}$ to filter out the stars that are not moving at similar speeds. Note that we choose this deviation value arbitrarily; raising or lowering it will control how strict our filtering is and affect our results. We find that ± 0.5 is a good threshold because we are left with 433 cluster members after filtering the queried stars. It is only necessary to do this process for one calibrated science image of Mel 71, such as that in Figure 2.

3.4. *Astrometry and Aperture Photometry*

After finding the RAs and DECs of 433 cluster members, we now take steps to map their locations onto our calibrated images in order to perform photometry on each of them. First, we submit our 60 s, V band image of Mel 71 to Astrometry.net. This tool identifies the stars in the image and returns a "wcs.fits" file. The file uses the World Coordinate System (WCS) convention which maps world coordinates, RA and DEC, to the pixels of an N-dimensional image.[7] We specifically need the CRVAL, CRPIX, and CD information from the header of the FITS file. These values allow us to

[7] Jaffe T., 2021, FITS World Coordinate System

transform from RAs and DECs to pixel coordinates on our image.

Before transforming coordinates, we convert our RAs and DECs into units of hour angle and degrees respectively using SkyCoord. This is a necessary step otherwise the transformation will not work. With the arrays of the converted RAs and DECs, we then create a WCS object using the important header information from the FITS file and use the method $wcs\_world2pix()$ to return arrays for the corresponding x and y pixel coordinates. This method requires three arguments, with two being the RA and DEC arrays. The third is most important, which we set to 0 in order to get the transformation to function properly. These x and y pixel coordinates are relatively accurate, as seen when plotted over our cluster image in Figure 3. Before continuing, note that we repeat the entire process we outline in this section for a 60 s, B band image of Mel 71 as well.

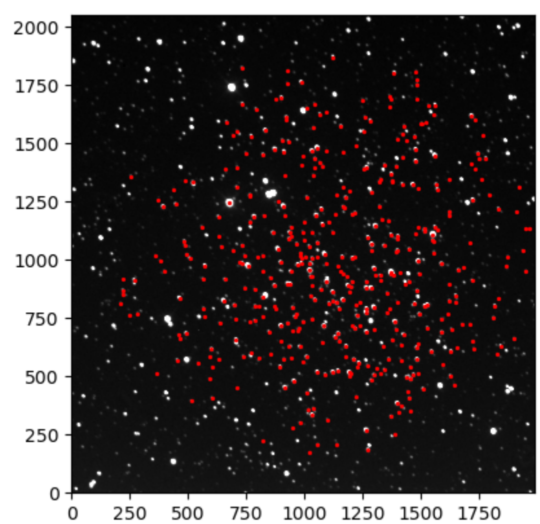

Figure 3. X and Y centroids of each cluster member plotted on top of a 60 s, V band exposure of Mel 71. Note that the orientation is North down, East right.

Now that we know the x and y coordinates of the stars in the cluster, we use $photutils$ to define both a circular aperture around each star and an annulus just outside of the aperture. We use the aperture to calculate the total flux in counts of the target star, while the annulus allows us to collect the total flux of the sky background. It is important that the aperture completely encloses the target star and that the annulus is at a location where the sky flux it measures is not affected by nearby light sources. For each star, we set the aperture radii to 12 and the annulus radii from 13 to 18. An example of the aperture set up is pictured in Figure 4.

With our apertures and annuli set, we calculate the total counts from each star and sky background separately using $photutils.do\_photometry()$. These values are the star sum

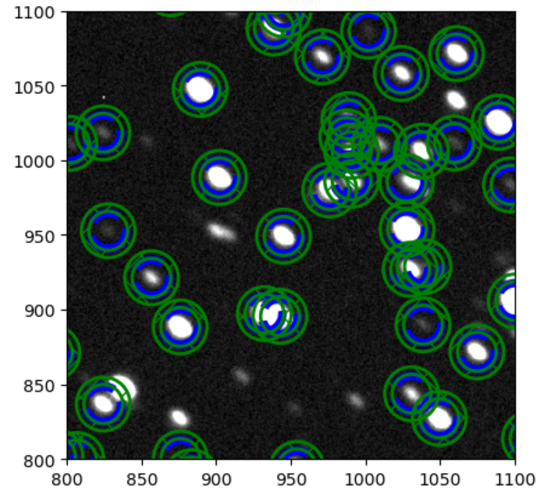

Figure 4. A 300x300 subframe of a 60 s, B Band image of Mel 71 with the apertures plotted over the cluster stars. Note that some apertures overlap, which is a problem which we address.The orientation is North down, East right.

and sky sum respectively. We then divide the sky sum by the area of the annulus to get the average sky counts per pixel. Lastly, we multiply the average sky by the area of the aperture and subtract the resulting value from the star sum. This process results in a sky-subtracted star sum for each star in the cluster, which we can now use to find their apparent magnitudes.

To calculate the apparent magnitudes in the B and V bands for each star, we first need the known apparent magnitude of a star in our images. We use MMU 130 as our comparison star which has SIMBAD reported magnitudes of V = 12.687 and B = 13.786. Next, we define a flux ratio for each star in the cluster by dividing their sky-subtracted star sum by the star sum of MMU 130. With these values, we use the following equation to calculate the apparent magnitudes:

$$m = -2.5log(F_R) + m_{comp} \tag{1}$$

Where m is the apparent magnitude in either the B or V band, F_R is the flux ratio defined above, and m_{comp} is the magnitude of the comparison star in either band. Through this process, we calculate the B and V apparent magnitudes for each star in the cluster. It is important to note that some of the stars are not bright enough to produce counts above the sky background. The magnitudes we calculate for these stars end up returning NaN objects. To quickly remedy this, we set these undefined magnitudes to 0 which we filter out when creating our CMD. This issue results in a loss of the information of 40 stars, bringing our total cluster count down to 393 stars.

3.5. *Color-Magnitude Diagram*

Using the arrays of the B and V magnitudes we find in section 3.4, we simply subtract the two to obtain the $(B-V)$ color index for each star. We then create a scatter plot with V against $(B-V)$ to produce a CMD for Mel 71, as seen in Figure 5. We observe a main sequence turnoff point at $(B-V) = 0.35$ and apparent V magnitude of 13 as well as a branch of red giants from $(B-V) = 0.6$, $V = 13$ to $(B-V) = 1.2$, $V = 10$. Note that we find these values by eye rather than by mathematical means.

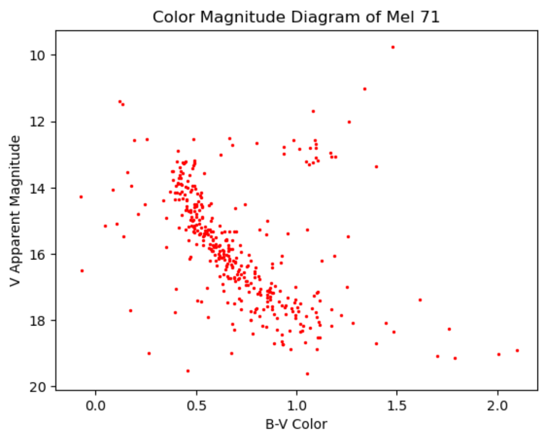

Figure 5. Our CMD for Mel 71 with apparent V magnitude plotted against $B-V$ color. The main sequence structure has a turnoff point at $(B-V) = 0.35$. There is also branch of red giants from $(B-V) = 0.6$ to $(B-V) = 1.2$. A total of 393 stars are plotted.

4. DISCUSSION

The CMD we create in Figure 5 seems to be a relatively accurate observational isochrone for Mel 71. There is a distinct main sequence phase and turnoff point at $(B-V) = 0.35$ and $V = 13$, as well as an asymptotic branch of stars from magnitudes of V = 13 and brighter. The turnoff index we find is slightly redder than that in the work of Pound-Janes, where they report an index of $(B-V) = 0.28$. We believe this discrepancy is due to the difference in data observed and the fact that we report the turnoff point by eye, so there is significant room for error. We also note that the shape of our CMD matches the general shape for open cluster CMDs.

When looking at the branch stars, which share a similar range of $(B-V)$ colors from 0.35 to 1.25 as the main sequence stars, they are typically brighter. These stars must be more massive than the main sequence stars in order to account for their higher brightness, which leads us to believe that these are red giants. These stars are most likely the most massive stars born in Mel 71 and evolve off the main sequence much quicker than their lower mass siblings. This observation is in line with the findings of Pound-Janes, where they take note of a ”red giant clump” that stems off the main sequence turnoff point in their CMD. Further, this red giant branch is analogous to the horizontal branch that we see in the CMDs of globular clusters, meaning that Mel 71 is most likely an older open cluster.[8]

While our CMD is a good illustration of the effects of stellar evolution on Mel 71, the process we outline in section 3 has issues that potentially affect our results. The first lies within the fact that we only use proper motion as a criteria for cluster membership. Since stars in a cluster are born from the same interstellar cloud, they will have similar chemical compositions in addition to moving at roughly the same speed. So, using spectral or photometric data alongside proper motion may increase the accuracy of our filtering. While a potential fix, this filtering system may actually be too strict and weed out stars that are indeed part of the cluster.[9] For Mel 71, using only proper motion as membership criteria is accurate enough to create a good CMD.

The other issue stems from our use of photometry. In Figure 4, it is plain to see that a number of the apertures overlap with each other. This overlapping results in unreliable star and sky sums for some stars that affect the apparent magnitudes that we calculate. The effects of this issue can be seen in our CMD in Figure 5, where there are a number of stars that deviate far from the defined main sequence and red giant branch. These outliers are most likely stars in dense regions of the sky we are observing where the overlapping of apertures around the stars is an unavoidable problem. While we can filter out these stars in our process, this issue does not affect the overall stellar evolution in our CMD.

5. SUMMARY

In this lab, we produce a CMD for the open cluster Mel 71 that accurately illustrates the effects of stellar evolution on similar age stars with different masses. We outline a method in section 3 that astronomers can reproduce to create CMDs for other open clusters, not just Mel 71, given they have the necessary observational data. It is important to note that our photometric methods will most likely not work with globular clusters, as they are much more dense compared to open clusters. We also highlight the potential shortcomings of our methodology, which any astronomer may improve on to create a more accurate CMD, much like how we update the CMD of Pound-Janes.

We report a main sequence turnoff index of $(B-V) = 0.35$ and observe a red giant branch on our CMD. The defined main sequence and red giant regions of Mel 71 show that some of the more massive stars in the cluster have evolved off the main sequence already. This observation implies that

[8] Pound, M. W. and Janes K. A., 1985, The Intermediate-Age Open Cluster Mel 71 (Department of Astronomy, Boston University)

[9] Stott J. J., 2018, Determining open cluster membership - A Bayesian framework for quantitative member classification.

Mel 71 is most likely an older cluster; the older it gets, the more stars there will be in the red giant branch.

In order to improve and further our work, we can perform either a chi-squared or a zero-age main sequence (ZAMS) fit on our CMD data to obtain a more accurate isochrone for Mel 71. This modelled isochrone will report the main sequence turnoff index and red giant branch region to a better degree of accuracy than doing it by eye. We can also follow in the footsteps of Pound-Janes, where they use the red giant branch to find the reddening, distance, and age of the cluster. This is done using a comparison open cluster with a well established isochrone like Hyades. With these values, we can correct our CMD for reddening to produce the most accurate data possible. The more accurate our CMDs are, the better our models of stellar evolution will become.

Thanks to my group members Jacqueline, Paulina, and Ariyana for the collaborative work on creating the CMD for this lab as well as the observation logs we reference for this lab report. Massive thanks to the Perkins Telescope Observatory and specifically Colt for assisting us with remote observations after we were unable to do any during the Arizona trip.

Facilities: Perkins Telescope Observatory and PRISM

Software: Astrometry.net, astropy, astroquery, glob, matplotlib, numpy, pandas, photutils, scipy, SIMBAD, WCS

6. REFERENCES

Australia Telescope National Facility, Open Star Clusters

Boston University, Perkins Observatory Instruments

GAIA in the UK, Star clusters: observing the effects of stellar evolution

Harvard and Smithsonian Center for Astrophysics, Star Clusters

Jaffe T., 2021, FITS World Coordinate System

Lang, D., Hogg, D. W.; Mierle, K., Blanton, M., & Roweis, S., 2010, Astrometry.net: Blind astrometric calibration of arbitrary astronomical images, Astronomical Journal 137, 1782–1800. http://arxiv.org/abs/0910.2233

Pound, M. W. and Janes K. A., 1985, The Intermediate-Age Open Cluster Mel 71 (Department of Astronomy, Boston University)

Stott J. J., 2018, Determining open cluster membership - A Bayesian framework for quantitative member classification.